Supercurrent without a spatially varying phase or a vector potential from time-reversal and inversion symmetries breaking in superconductors

Daniel Palacios, Pavan Hosur[1]

[1]*Department of Physics, University of Houston, Houston 77204, USA*

Non-conventional superconductivity when time-reversal and inversion symmetries are violated in non-centrosymmetric superconductors is investigated. Superconductors require a phase difference in order to conduct a nonzero current, this would not be true in an asymmetric superconductor. The Josephson effects were also derived for this novel type of superconductors. Numeric calculations are also performed by determining the super-current density in 2D and 3D lattices. FFLO superconductivity is also explored for this type of superconductors. Modern computational techniques like image recognition were deployed to make the models automated as much as possible.

I. INTRODUCTION

A. Background

Superconductivity is one of the greatest frontiers of scientific research and is responsible for cutting-edge technology. The superconducting state allows materials to lose electrical resistance and have a current flowing without energy dissipation, which is known as a supercurrent. The transition to this state permits for phenomena like the Meissner effect. Materials transition to a superconducting state when the effective net attraction between the electrons produces a weak pair binding energy at extremely low temperatures. These pairs are known as Cooper pairs. The effective net attraction between electrons emerges from the phonon interaction with the metal lattice. In normal conductors, electrons lose energy from scattering, but Cooper pairs behave like bosons that condense into the same state and do not scatter as single electrons. For a supercurrent to be generated in this state, it requires a spatially varying phase. One way of achieving this is through a Josephson junction which consists of two pieces of superconducting material separated by a thin, insulating barrier where Cooper pairs have the property of quantum tunneling, creating an electric current, known as Josephson's current or Josephson effect. Asymmetric superconductors, in which time-reversal symmetry and inversion symmetry are broken, promise to generate a supercurrent without a phase or vector potential.[1] Superconductors have a large variety of important technological applications. For example, when superconducting electromagnets are used in magnetic resonance imaging and maglev trains. Asymmetric superconductors could have useful properties for electronics, in particular, they promise to be candidates for superconducting diodes and will carry much larger currents than existing semiconductor diodes. Inversion symmetry and time-reversal symmetry are required for the formation of Cooper pairs which occurs in symmetrical superconductors. The simultaneous breaking of these symmetries leads to the creation of an asymmetric superconductor. Forming Cooper pairs when both symmetries are broken is difficult. However, it is important to study asymmetric superconductors to better understand nonconventional superconductivity. The behavior of a supercurrent density in these materials is not well understood. In this project, I derived an analytical expression for the expectation value of the supercurrent in asymmetric superconductors which shows the existence of a supercurrent in the absence of a phase or vector potential. I also explore the nature of this materials in Josephson junctions. Some materials could exhibit this condition such as the non-centrosymmetric, magnetic heavy-fermion superconductor CePt3Si. [2]

1. *BCS Theory*

When electrons travel to materials, energy is dissipated in form of heat due to electrical resistance. A superconductor is a metal which at a critical temperature it looses all its electrical resistance. This state allows a current to flow without energy dissipation. Superconductor has varied applications, the most popular one is the use of superconducting materials to create large magnetic fields to accelerate particles at the Large Hadron Collider. Other applications include strong MRI machines, and fast levitating trains (Meglev Train). Bardeen–Cooper–Schrieffer theory has been the main way superconductivity is understood. Electrons are fermions, and they like being in different energy states obeying Pauli's Exclusion principle. However, at very low temperature, electrons form pairs due to the phonon lattice interactions (shown in Figure 1). This new form pairs call Cooper pairs stop being fermions, and they behave like bosons. Cooper pairs not longer have to obey Pauli's exclusion principle, and they can take the same state. In fact, they form a condensate take the lowest possible energy state.[3–7]

2. *Second Quantization*

First quantization, refers to the transformation from classical mechanics to quantum mechanics i.e. the transformation of the classical Hamiltonian to an operator, $\hat{H}$. This results in the Schrodinger equation ($i\hbar\partial_t\psi = \hat{H}\psi$) which

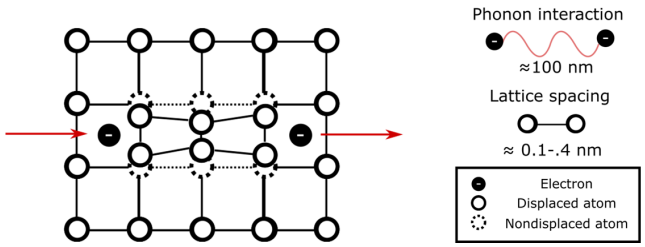

Figure 1. Cooper pairs are form from moving electrons in a lattice attracts the positive ions, another electron far away is attracted to the collective motion of the positive charged lattice (phonon). Net attraction between cooper pairs is very weak, and small thermal agitation is needed to convert them back to normal electrons.

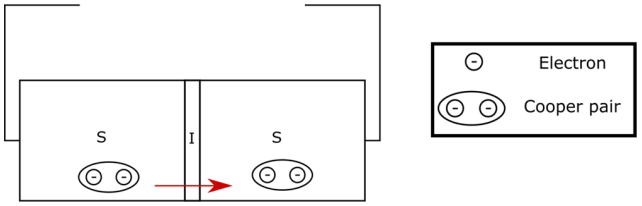

Figure 2. Classic Josephson junction (SIS) consists in a Superconductor-Insulator-Superconductor configuration Cooper pairs quantum tunnel through the insulator to generate a super-current.

describes the evolution of the wave-function. This approach is very successful when the number of particles is fixed and when they describe one body problems. However, when many particles are consider, the use of the Schrodinger equation becomes unpractical. The reformulation of quantum mechanics to deal with many body interacting particles problems is called Second Quantization. In this formulation, occupation number represents indistinguishable particles, and creation–annihilation operators increase or decrease the number of particles. [8]

3. *Josephson junctions*

A classical Josephson junction consists of two superconducting layers separated by a thin insulator (shown in Figure 2). DC or AC currents can be generated by quantum tunneling trough the thin barrier. Josephson junctions appear to be good candidates for the creation of qubits from the developing of quantum computers. Josephson junction can also be arrange in other configurations to form superconducting quantum interference device – SQUID. These devices are very sensible to magnetic fields. [1, 9, 10]

4. *Fermi-surface and energy dispersion*

In solid state physics, the transport property of materials are characterized by the energy dispersion near the Fermi surface. Measurements of transport properties provide information on the energy dispersion behavior. Generally, these measurements are considered fundamental since they can be performed in most solids and can be used to distinguished material. The energy dispersion is specially important in defining the Fermi-surface of a metal. [11] Since electrons in a metal obey the Pauli's exclusion principle, they occupied different states. For a defined number of electrons they fill up the lowest possible states to form a Fermi-sea. The outermost layer of this electron sea is called the Fermi-surface. Electrons considerably below the Fermi-surface can not get easily excited and contribute to the transport property of the material. The shape and features of the Fermi-surface are important to describe phenomena such as the ability of electrons to screen perturbations, superconductivity, oscillatory exchange coupling, and others. [12]

5. *Mean-field Theory and Bogoliubov-de Gennes Transformations for Superconductivity*

Mean-field theory is an approximation to reduce the number of degrees of freedom of complex systems by studying simpler systems. In solids, MFT makes significant contributions when predicting phase transitions since each particle has many nearest neighbors. In order to utilize mean-field theory, an interacting Hamiltonian model is needed where correlation effects are neglected, additionally, the mean-field theory Hamiltonian has to be solved by self-consistency equations. [13]

Bogoliubov-de Gennes Hamiltonian can be obtained by imposing mean-field approximation in the Superconductivity Hamiltonian and considering first order terms. This matrix can be easily diagonalized since it is Hermitian.[14]

6. *The Fulde-Ferrell-Larkin-Ovchinnikov (FFLO) state in superconductivity*

Layered organic superconductors can be modeled as a system of stacked Josephson Junctions. When a parallel applied field interacts with the layers, the orbital effect becomes strongly quenched. The clean-limit superconductivity and quenched orbital effect provide the conditions necessary to create a new superconducting, SC, phase. This state is known as the Fulde-Ferrell-Larkin-Ovchinnikov (FFLO) phase. [15]

The splitting of spectral lines when an atom is placed in an external magnetic field is known as the Zeeman effect. This effect imposes an upper limit on the critical magnetic field of conventional spin-singlet superconductors, known

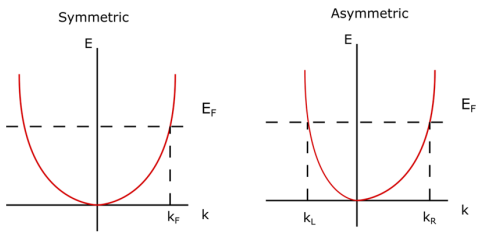

Figure 3. (Left) Energy dispersion for a symmetric metal, the fermi energy (E_F) corresponds to a fermi momentum (k_F). (Right) Energy dispersion for an asymmetric metal, here the fermi energy corresponds to two different values of the fermi momentum (left and right fermi momentum - k_L and k_R).

as the Pauli (or Clogston-Chandrasekhar) limit. However, the FFLO state can occur even above Pauli limit sufficiently below T_c in parallel fields. Consequently, the FFLO transition for a conventional superconducting phase is expected to exist at the Pauli limit. During this state, the Cooper pairs are made of the opposite spins which live in the polarized Fermi surface. [16]

B. Motivation

Inversion symmetry and time reversal symmetry are required for the formation of Cooper pairs which occurs in symmetrical superconductors. [17] The simultaneously breaking of these symmetries leads to the creation of an asymmetric metal. When this metal turns superconducting, the resulting superconductor is an asymmetric superconductor.

Consider a one dimensional symmetrical energy dispersion, the Fermi-energy is the same for a left momentum ($-k$) and right momentum ($+k$). However, for a one dimensional asymmetric energy dispersion, this is not true, since $|-k| \neq |k|$. From this fact, a current density($\propto E(-k) - E(k)$) for the symmetric case is clearly zero, however, for the non symmetric case it is expected a nonzero energy difference. This difference can be visualized in Figure 3 and is a hint for a nonzero super-current.

Rudimentary analytic calculations with second quantization operator algebra was done to calculate the expectation value of the super-current for an asymmetric superconductor considering the BdG Transformation. Similar calculations were done with Matrix operation for a zero temperature approximation and finite nonzero temperatures. Detailed calculations and notes are shown in Appendix A.

II. METHODS

A. Schrodinger equation for an asymmetric superconductor

Consider the following Schrodinger equation of a charged particle in a magnetic field with an asymmetric energy dispersion:

$$i\partial_t\psi = [\frac{(\hat{p} - q\mathbf{A})^2}{2m} - a(\hat{p} - q\mathbf{A}) + q\phi]\psi \tag{1}$$

From the Schrodinger equation the super-current density phase relation and the energy phase relation can be obtained (details are shown in Appendix A). Then these two expressions are used to derive the Josephson effects.

The London equations can also been analytically solved by the Schrodinger equation results. Since we consider a linear asymmetric term, the second London equation leads to the original Meissner effect for both symmetric and asymmetric superconductors. In the other hand, a different expression is found for the first London equation which is shown in Appendix A.

The Conventional DC Josephson effect is:

$$J = J_c sin(\phi) \tag{2}$$

Where J_c is the maximum critical current and ϕ is the Josephson phase. A DC current exist due to quantum tunneling if there is a spatially phase difference across the junction, even in the absence of a potential difference. After deriving the current and energy phase relations for the asymmetric case, the Asymmetric DC Josephson effect obtained is:

$$J = J_c sin(\phi) + J_m cos(\theta) + aqn \tag{3}$$

Where a corresponds to the asymmetric coefficient, q is the charge, and n the particle density. In contrast to the symmetric case, for asymmetric superconductors there exist a current even if the Josephson phase vanishes. Other main Josephson effect can be obtained in similar fashion. The AC Josephson effect is:

$$J(t) = J_c sin(\frac{2\pi}{\Phi_0}Vt) + J_m cos(\frac{2\pi}{\Phi_0}Vt) + aqn \tag{4}$$

while the Inverse AC Josephson effect is:

$$\begin{aligned} I = I_c(\sum_{k=-\infty}^{\infty} J_k(\alpha))sin(\phi_0 + \rho\omega t + k\omega t)) \\ +I_m(\sum_{k=-\infty}^{\infty} J_k(\alpha)cos(\phi_0 + \rho\omega t + k\omega t)) + aqn \end{aligned} \tag{5}$$

In the AC Josephson effect, a constant voltage, V, is applied, generating an oscillating current. In an asymmetric superconductor the current would be shifted by the asymmetric contribution of the super-current. In the inverse AC Josephson effect microwave radiation induces quantized DC voltages. It is expected a similar effect for asymmetric

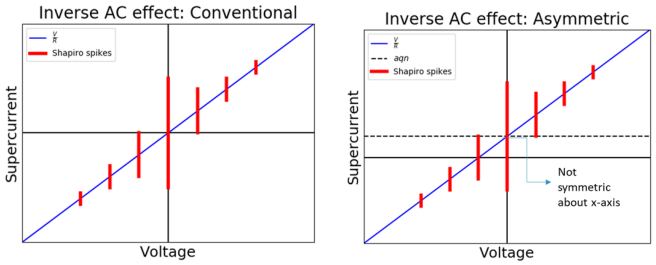

Figure 4. Conventional Inverse AC effect. Shapiro spikes for a conventional superconductor, specific voltage values causes a jump in the current. Asymmetric Inverse AC effect. Shapiro spikes for an asymmetrical superconductor.

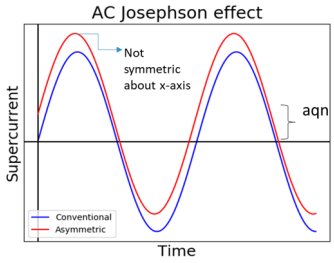

Figure 5. AC Josephson Effect plot Current vs Time illustrating the AC Josephson effect, in a constant voltage asymmetric and conventional super-current oscillate sinusoidally

superconductors with a constant shift in an I-V plot. The difference between the symmetric and asymmetric case in the Inverse AC effect is shown in Figure 4 where the current is not symmetric about the x-axis. A similar shift is displayed on Figure 5 for the AC Josephson effect where the current is vertically translated by the asymmetric term.

The energy of an asymmetric basic junction can also be calculated. As well as similar expressions, the asymmetric term carries linearly through the calculations. Ginzburg-Landau theory [18] calculations were similarly calculated for asymmetric superconductors by incorporating an asymmetric term in the free enthalpy (details for energy calculations and Ginzburg-Landau equations are shown in Appendix A).

B. Deriving an asymmetric energy dispersion for a lattice

Understanding about Bloch Theorem describes that no fermionic system can have a non-zero current [19]. However, in finite lattices there can still be a non-zero supercurrent[20]. The lattice energy dispersion for asymmetric superconductors by considering 2 types of hopping terms (shown in Figure 6) can be derived. This was necessary since the system conserved time-reversal symmetry under Gauge-transformation. In other words, the condition of $t \in \mathbf{C}$ is not sufficient for time-reversal symmetry breaking.

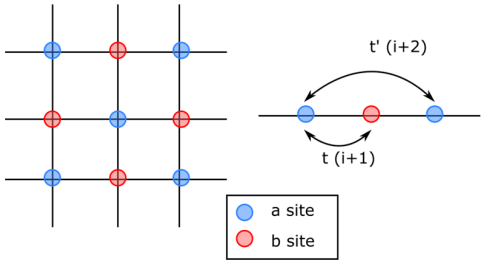

Figure 6. 2D Square lattice with 2 types of hopping terms. Note a and b sites do not represent different atoms. The odd hoppings between a and b sites are represented with t', while even hoppings are between a sites are represented with t.

From this logic, a tight-binding Hamiltonian for an asymmetric superconductor is obtained:

$$H = -\frac{1}{2}\sum_{i,\sigma}\sum_{\delta}(te^{i\theta}c^{\dagger}_{i\sigma}c_{i+\delta,\sigma} + te^{-i\theta}c^{\dagger}_{i+\delta,\sigma}c_{i\sigma} + t'e^{i\phi}c^{\dagger}_{i\sigma}c_{i+2\delta,\sigma} + t'e^{-i\phi}c^{\dagger}_{i+2\delta,\sigma}c_{i\sigma}) + VN \tag{6}$$

From the Hamiltonian we get the energy dispersion for an asymmetric superconductor by transforming the equation to k-space. After a Gauge transformation this yields:

$$\xi_k = tcos(ka) + t'cos(2ka + \tilde{\theta}) \tag{7}$$

Where the phase angle, $\tilde{\delta}$, breaks inversion symmetry. It is important to note that symmetry is recovered when the angles in their respective direction vanish.

C. Quantifying asymmetric super-current density in a lattice

Defining the expectation of the super-current density as:

$$\langle J \rangle = tr[U_k P_k U_k^{\dagger} \hat{J}_k] \tag{8}$$

Where U_k and $U_k^{\dagger}$ are the unitary Bogoliubov-de Gennes Transformations from a Hamiltonian with superconductivity. The projection matrix operator, P_k, is a diagonal matrix with Fermi-Dirac functions (or step functions at the zero temperature approximation). The super-current matrix operator, J_k, corresponds to a diagonal matrix with the first derivative of the energy dispersion. Details can be found in Appendix A. After applying periodic boundary conditions, the total super-current can be given by:

$$\langle J \rangle = \frac{1}{V}\sum_{n_x n_y n_z}\langle j_k \rangle \tag{9}$$

The equation above can be solve numerically to calculate the super-current density and analyze the dependency of it respect to different parameters.

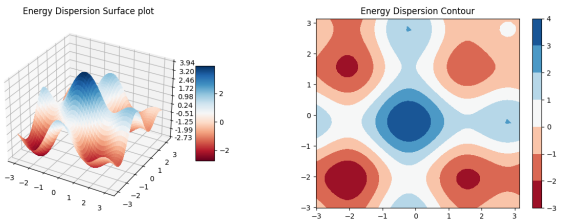

Figure 7. (Left) Asymmetric Energy dispersion surface plot. This is obtain by a grid on equation (7). (Right) Asymmetric Energy dispersion contour plot. Similarly, it represents the shape of equation (7)

D. Asymmetric FFLO state

Phase transitions can be found by minimizing the Helmholtz free energy. The Helmholtz free energy for an asymmetric FFLO superconductor is:

$$F = -\frac{N}{2V_0}\sum_k |\Delta_{2k}|^2 + \sum_{s;E_s>0} lncosh(\beta E_s) \qquad (10)$$

Where E_s are the eigenvalues of the BdG Hamiltonian which are obtaied numerically after the diagonalization of h i.e. $h\,|s\rangle = E_s\,|s\rangle$. N refers to the number of particles, V_0 is the potential, Δ_{2k} corresponds to the nonzero contributors of the BdG Hamiltonian. While β is the thermodynamic beta.

To create the BdG FFLO Hamiltonian matrix all momentum pairs have to be indexed after applying periodic boundary conditions. After that, a contour is drawn numerically when the energy dispersion is zero which corresponds to the fermi-level. For an asymetric energy dispersion these contour takes the form after interpolation shown in Figure 8. These contour helps to identify fermi-surface nesting. Fermi surface nesting occurs when parts of a Fermi surface are connected to another part of another Fermi surface via the reciprocal lattice vector. These fermi-surface segments or parts tend to be straight lines. Fermi surface nesting is important to identify nonzero Δ pairs in the BdG FFLO Hamiltonian matrix. From the contour $k + k'$ momentum pairs are calculated and a 2D histogram is constructed (shown in Figure 9). The peaks of this histogram are evidence of fermi-surface nesting, and the contributor pairs which are come pre-indexed are used to construct the BdG FFLO Hamiltonian matrix. The other Δ pairs are set up to zero since they do not contribute and make the numerical solution of the eigenvalues easier. Since this matrix is size $4N \times 4N$, they become large fairly quickly as the lattice size increases.

The peaks of the histogram could be identify manually by passing the important k_x and k_y coordinates and extracting the important indexed pairs. However, doing this every time the model is run can be time draining. To avoid this a machine learning algorithm in image recognition was used (shown in Figure 10). Since a 2d histogram is analog

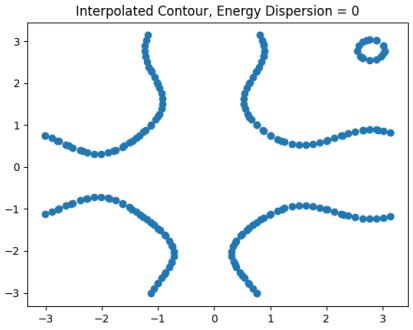

Figure 8. Interpolated contour plot at the fermi-level. Contour lines can be obtained by setting up the energy dispersion to an specific value. In particular at zero, is where most of the physics occur. Numerically, the precision of this contour depends on the number of points which is proportional to the lattice size. In order to draw a continous contour points are interpolated. However, since they are indexed, they cannot be used to calculate for nesting. The non-interpolated contour is prefered by selecting a small range of values close to zero.

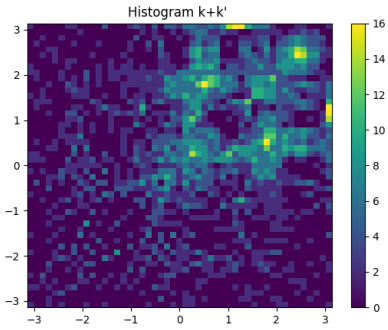

Figure 9. All possible $k + k'$ pairs in the contour are calculated. These values are plot in this 2D histogram, the peaks correspond to important contributor momentum pairs which are evidence of fermi-surface nesting. These coordinates have specific Δ pairs associated with it which are saved to construct the BdG Matrix to calculate the Helmholtz free energy in later calculations.

to an image, a feature image recognition model can easily extract the peaks of the histogram. The developed model constructs the Hamiltonian BdG FFLO matrix with given energy dispersion. This energy dispersion could be symmetric or asymmetric. The parameters of the energy dispersion are also inputs of the model. Consequently, the model can identify nesting, extract the important momentum pairs automatically, construct the matrix of interest, and calculate the Helmholtz free energy.

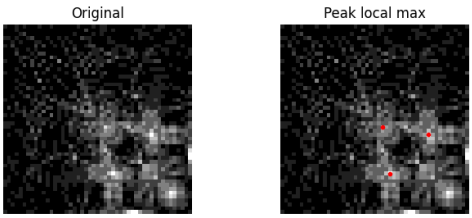

Figure 10. (Left) Pre-processed histogram image passed to the machine learning image feature recognition algorithm from scikit [21]. (Right) automatic identification by machine learning algorithm, three identified peaks are highlighted in red, and coordinates are identified.

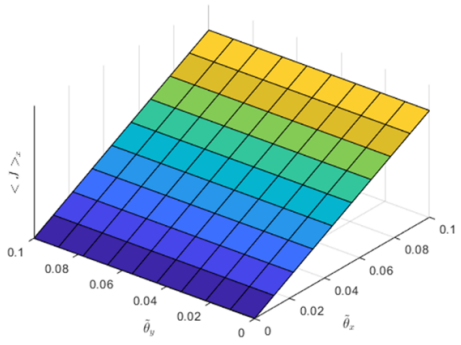

Figure 11. Expectation value of the supercurrent density in the x direction vs. asymmetry angles x and y plot.

III. DISCUSSION AND RESULTS

The model (super-current density) was calculated numerically and tested across several parameters. There is a constant super-current across different lattice sizes and a linear relation across small asymmetry angles. The super-current in the x-direction is plotted as a function of the asymmetry in Figure 11. When the asymmetric angles of the super-current are zero, the system recovers symmetry, and the asymmetric contribution of the super-current vanishes. Similar behavior was obtained from 3D simple cubic lattice.

Inducing an asymmetry on non-centrosymmetric superconductors would allow to have a supercurrent without the need of a spatially varying phase even if we assume a small asymmetry. Inducing superconductivity on asymmetric metals turns out to be challenging, one idea is to induce superconductivity extrinsically by putting an asymmetric metal next to a conventional superconductor. The model for the calculation of the super-current in a 3D lattice showed a non-zero super-current across many parameters.

IV. FUTURE WORK

Investigate ring geometry in superconductors to explore the possibility of calculating numerically the super-current density in asymmetric ring superconductors. Complex gaps can be considered by modifying the BdG Hamiltonians from the models presented in this paper.

It also necessary to verify the results of the FFLO asymmetric model and compare to literature[22] in order to replicate phase transition diagram. Then parameters of interest can be modify to scan properties of asymmetric superconductors and compare directly with symmetric energy dispersions. Identify asymmetric metals that can be good candidates to create this non-conventional superconductors is also important in order to design experiment to compare to ideas presented in this paper, some candidates are [cite here].

After obtaining a Mean Field theory approximation for FFLO state, it can be possible to explore more sophisticated models involving Monte Carlo simulations, and quantum AI algorithms to simulate other physical phenomena of these systems.

We acknowledge financial support from the Summer Undergraduate Research Fellowship and Provost's Undergraduate Research Scholarship Programs funded through the Office of Undergraduate Research and Major Awards.

[1] Manfred Sigrist. Introduction to unconventional superconductivity in non-centrosymmetric metals. In *AIP Conference Proceedings*, volume 1162, pages 55–96. American Institute of Physics, 2009. I A, I A 3

[2] Youichi Yanase and Manfred Sigrist. Superconductivity and magnetism in non-centrosymmetric system: application to cept3si. *Journal of the Physical Society of Japan*, 77(12): 124711–124711, 2008. I A

[3] Pierre-Gilles De Gennes and Philip A Pincus. *Superconductivity of metals and alloys*. CRC Press, 2018. I A 1

[4] Takafumi Kita. *Statistical Mechanics of Superconductivity*. Springer, 2015.

[5] Hiroyasu Koizumi. Theory of supercurrent generation in bcs superconductors. *arXiv preprint arXiv:1810.12508*, 2018.

[6] John Bardeen, Leon N Cooper, and John Robert Schrieffer. Theory of superconductivity. *Physical review*, 108(5):1175, 1957.

[7] Michael Tinkham. *Introduction to superconductivity*. Courier Corporation, 2004. I A 1

[8] FA Berazin. *The method of second quantization*, volume 24. Elsevier, 2012. I A 2

[9] Philippe Mangin and Rémi Kahn. *Superconductivity: an introduction*. Springer, 2016. I A 3

[10] D Singh, PK Biswas, AD Hillier, RP Singh, et al. Superconducting properties of the noncentrosymmetric superconductor laptge. *Physical Review B*, 98(21):214505, 2018. I A 3

[11] Riichiro Saito, Ado Jorio, Antonio Gomes Souza Filho, Gene Dresselhaus, MS Dresselhaus, and Marcos Assunção

Pimenta. Probing phonon dispersion relations of graphite by double resonance raman scattering. *Physical review letters*, 88(2):027401, 2001. I A 4

[12] Stephen B Dugdale. Life on the edge: a beginnerâs guide to the fermi surface. *Physica Scripta*, 91(5):053009, 2016. I A 4

[13] Paul M Chaikin, Tom C Lubensky, and Thomas A Witten. *Principles of condensed matter physics*, volume 10. Cambridge university press Cambridge, 1995. I A 5

[14] Jian-Xin Zhu. *Bogoliubov-de Gennes Method and Its Applications*, volume 924. Springer, 2016. I A 5

[15] AB Kyker, WE Pickett, and F Gygi. Fermiology and fulde-ferrell-larkin-ovchinnikov phase formation. *Physical Review B*, 71(22):224517, 2005. I A 6

[16] Shiori Sugiura, Takayuki Isono, Taichi Terashima, Syuma Yasuzuka, John A Schlueter, and Shinya Uji. Fulde–ferrell–larkin–ovchinnikov and vortex phases in a layered organic superconductor. *npj Quantum Materials*, 4(1):1–6, 2019. I A 6

[17] D Singh, KP Sajilesh, S Marik, AD Hillier, and RP Singh. Superconducting properties of the noncentrosymmetric superconductor taos. *Superconductor Science and Technology*, 30(12):125003, 2017. I B

[18] M Cyrot. Ginzburg-landau theory for superconductors. *Reports on Progress in Physics*, 36(2):103, 1973. II A

[19] David Bohm. Note on a theorem of bloch concerning possible causes of superconductivity. *Physical Review*, 75(3): 502, 1949. II B

[20] Haruki Watanabe. A proof of the bloch theorem for lattice models. *Journal of Statistical Physics*, 177(4):717–726, 2019. II B

[21] Stefan Van der Walt, Johannes L Schönberger, Juan Nunez-Iglesias, François Boulogne, Joshua D Warner, Neil Yager, Emmanuelle Gouillart, and Tony Yu. scikit-image: image processing in python. *PeerJ*, 2:e453, 2014. 10

[22] Yann Claveau, Brice Arnaud, and Sergio Di Matteo. Mean-field solution of the hubbard model: the magnetic phase diagram. *European Journal of Physics*, 35(3):035023, 2014. IV

Appendix A: Important derivations and other key results

EXPECTATION VALUE OF THE SUPERCURRENT OF A ASYMMETRIC SUPERCONDUCTOR: OPERATOR METHOD

Considering:

$$\langle j_i \rangle = \frac{2e}{(2\pi)^d} \int d^d k \partial k_i H_{BdG}(k) \left\langle c^\dagger_{k\uparrow} c_{k\uparrow} \right\rangle + \left\langle c^\dagger_{k\downarrow} c_{k\downarrow} \right\rangle \tag{A1}$$

$$\left\langle c^\dagger_{k\uparrow} c_{k\uparrow} \right\rangle = \langle sc | c^\dagger_{k\uparrow} c_{k\uparrow} | sc \rangle \tag{A2}$$

Where:

$$|sc\rangle = \prod_{k_i} \gamma^\dagger_{k_i\downarrow} \gamma^\dagger_{k_i\uparrow} |0\rangle \tag{A3}$$

Using:

$$\gamma^\dagger_{k\uparrow} = u_k c^\dagger_{k\uparrow} - v^*_k c_{-k\downarrow} \tag{A4}$$
$$\gamma^\dagger_{k\downarrow} = v^*_k c_{k\uparrow} + u_k c^\dagger_{-k\downarrow} \tag{A5}$$
$$\gamma_{k\uparrow} = u^*_k c_{k\uparrow} - v_k c^\dagger_{-k\downarrow} \tag{A6}$$
$$\gamma_{k\downarrow} = v_k c^\dagger_{k\uparrow} + u^*_k c_{-k\downarrow} \tag{A7}$$

Since:

$$\gamma^\dagger_{k\downarrow} \gamma^\dagger_{k\uparrow} |0\rangle = u_k (u_k c^\dagger_{k\downarrow} c^\dagger_{k\uparrow} + v^*_k) |0\rangle \tag{A8}$$

$$\langle 0| \gamma_{k\uparrow} \gamma_{k\downarrow} = \langle 0| v_k (u^*_k c_{k\uparrow} c_{k\downarrow} + v_k) \tag{A9}$$

We can argue:

$$\prod_{k_i} \gamma^\dagger_{k_i\downarrow} \gamma^\dagger_{k_i\uparrow} |0\rangle \propto \prod_{k_i} (u_{k_i} c^\dagger_{k_i\downarrow} c^\dagger_{k_i\uparrow} + v^*_{k_i}) |0\rangle \tag{A10}$$

$$\langle 0| \prod_{k_i} \gamma_{k_i\uparrow} \gamma_{k_i\downarrow} \propto \langle 0| \prod_{k_i} (u^*_{k_i} c_{k_i\uparrow} c_{k_i\downarrow} + v_{k_i}) \tag{A11}$$

$$\left\langle c^\dagger_{k\uparrow} c_{k\uparrow} \right\rangle \propto \langle 0| \prod_{k_i} (u^*_{k_i} c_{k_i\uparrow} c_{k_i\downarrow} + v_{k_i}) \; | \; c^\dagger_{k\uparrow} c_{k\uparrow} \; | \; \prod_{k_i} (u_{k_i} c^\dagger_{k_i\downarrow} c^\dagger_{k_i\uparrow} + v^*_{k_i}) |0\rangle \tag{A12}$$

$$\left\langle c^\dagger_{k\uparrow} c_{k\uparrow} \right\rangle \propto [\langle 0| \prod_{ki \neq k} ((u^*_{k_i} c_{k_i\uparrow} c_{k_i\downarrow} + v_{k_i})(u_{k_i} c^\dagger_{k_i\downarrow} c^\dagger_{k_i\uparrow} + v^*_{k_i})) |0\rangle]$$
$$[\langle 0| (u^*_k c_{k\uparrow} c_{k\downarrow} + v_k) c^\dagger_{k\uparrow} c_{k\uparrow} (u_k c^\dagger_{k\downarrow} c^\dagger_{k\uparrow} + v^*_k) |0\rangle] \tag{A13}$$

$$\left\langle c^\dagger_{k\uparrow} c_{k\uparrow} \right\rangle \propto [\prod_{ki \neq k} (|u_{k_i}|^2 + |v_{k_i}|^2)][(|u_k|^2)] \tag{A14}$$

$$\left\langle c^\dagger_{k\uparrow} c_{k\uparrow} \right\rangle \propto |u_k|^2 \tag{A15}$$

From equation previous equations:

$$\left\langle c^\dagger_{k\uparrow} c_{k\uparrow} \right\rangle = u_k v_k |u_k|^2 \tag{A16}$$

Thus:

$$\langle j_i \rangle = \frac{2e}{(2\pi)^d} \int d^d k \partial k_i H_{BdG}(k) 2 u_k v_k |u_k|^2 \tag{A17}$$

Let d=1 for simplicity:

$$\langle j_i \rangle = \frac{2e}{\pi} \int dk \partial k H_{BdG}(k) u_k v_k |u_k|^2 \tag{A18}$$

$$\langle j_i \rangle = \frac{2e}{\pi} [H_{BdG}(k') - H_{BdG}(k)] u_k v_k |u_k|^2 \tag{A19}$$

$$\langle j_i \rangle = \frac{2e}{\pi} [\begin{pmatrix} \xi_{k'} & -\Delta_{k'} \\ -\Delta^*_{k'} & -\xi_{k'} \end{pmatrix} - \begin{pmatrix} \xi_k & -\Delta_k \\ -\Delta^*_k & -\xi_k \end{pmatrix}] u_k v_k |u_k|^2 \tag{A20}$$

$$\langle j_i \rangle = \frac{2e}{\pi} [E(k') - E(k)] u_k v_k |u_k|^2 \tag{A21}$$

EXPECTATION VALUE OF THE SUPERCURRENT OF AN ASYMMETRIC SUPERCONDUCTOR: MATRIX METHOD

Hamiltonian Matrix:

$$\hat{H} = \begin{pmatrix} \xi_{k\uparrow} & 0 & \Delta_k & 0 \\ 0 & \xi_{k\downarrow} & 0 & \Delta_k \\ \Delta_k^* & 0 & -\xi_{-k\downarrow} & 0 \\ 0 & \Delta_k^* & 0 & -\xi_{-k\uparrow} \end{pmatrix} \tag{A22}$$

with eigenvalues:

$$E_{k,1,\pm} = \frac{1}{2}(\xi_{k\uparrow} - \xi_{-k\downarrow} \pm \sqrt{(\xi_{k\uparrow} + \xi_{-k\downarrow})^2 + 4|\Delta_k|^2}) \tag{A23}$$

$$E_{k,2,\pm} = \frac{1}{2}(\xi_{k\downarrow} - \xi_{-k\uparrow} \pm \sqrt{(\xi_{k\downarrow} + \xi_{-k\uparrow})^2 + 4|\Delta_k|^2}) \tag{A24}$$

Using the Bdg transformations:

$$c_{k\uparrow} = u_k^* \gamma_{k\uparrow} + v_k^* \gamma_{-k\downarrow}^\dagger \tag{A25}$$

$$c_{k\downarrow} = u_k^* \gamma_{k\downarrow} - v_k^* \gamma_{-k\uparrow}^\dagger \tag{A26}$$

$$c_{-k\downarrow}^\dagger = u_k \gamma_{-k\downarrow}^\dagger - v_k \gamma_{k\uparrow} \tag{A27}$$

$$-c_{-k\uparrow}^\dagger = -u_k \gamma_{-k\uparrow}^\dagger - v_k \gamma_{k\downarrow} \tag{A28}$$

To diagonalize $\hat{H}$ we choose:

$$U = \begin{pmatrix} u_k^* & 0 & v_k^* & 0 \\ 0 & u_k^* & 0 & v_k^* \\ -v_k & 0 & u_k & 0 \\ 0 & -v_k & 0 & u_k \end{pmatrix} \tag{A29}$$

Respectively:

$$U^\dagger = \begin{pmatrix} u_k & 0 & -v_k^* & 0 \\ 0 & u_k & 0 & -v_k^* \\ v_k & 0 & u_k^* & 0 \\ 0 & v_k & 0 & u_k^* \end{pmatrix} \tag{A30}$$

We can show:

$$UU^\dagger = U^\dagger U = \mathbb{1} \tag{A31}$$

Resulting:

$$H = \sum_k (\gamma_{k\uparrow}^\dagger, \gamma_{k\downarrow}^\dagger, \gamma_{-k\downarrow}, -\gamma_{-k\uparrow}) \begin{pmatrix} E_{k,1,+} & 0 & 0 & 0 \\ 0 & E_{k,2,+} & 0 & 0 \\ 0 & 0 & E_{k,1,-} & 0 \\ 0 & 0 & 0 & E_{k,2,-} \end{pmatrix} \begin{pmatrix} \gamma_{k\uparrow} \\ \gamma_{k\downarrow} \\ \gamma_{-k\downarrow}^\dagger \\ -\gamma_{-k\uparrow}^\dagger \end{pmatrix} + C \tag{A32}$$

We define:

$$\langle j \rangle = tr[U_k P_k U_k^\dagger \hat{J}_k] \tag{A33}$$

At 0 K temperature P_k simplifies to:

$$P_k = \begin{pmatrix} \Theta(-E_{k,1,+}) & 0 & 0 & 0 \\ 0 & \Theta(-E_{k,2,+}) & 0 & 0 \\ 0 & 0 & \Theta(-E_{k,1,-}) & 0 \\ 0 & 0 & 0 & \Theta(-E_{k,2,-}) \end{pmatrix} \tag{A34}$$

Where Θ is the step function (Heavy side function).
If

$$\hat{J} = \begin{pmatrix} \partial\xi_{k\uparrow} & 0 & 0 & 0 \\ 0 & \partial\xi_{k\downarrow} & 0 & 0 \\ 0 & 0 & \partial\xi_{-k\uparrow} & 0 \\ 0 & 0 & 0 & \partial\xi_{-k\downarrow} \end{pmatrix} \tag{A35}$$

for a single state we get:

$$\begin{aligned}\langle j\rangle = \partial\xi_{-k\uparrow}(|u_k|^2\Theta(-E_{k,1,-}) + |v_k|^2\Theta(-E_{k,1,+})) \\ + \partial\xi_{-k\downarrow}(|u_k|^2\Theta(-E_{k,2,-}) + |v_k|^2\Theta(-E_{k,2,+})) \\ + \partial\xi_{k\uparrow}(|u_k|^2\Theta(-E_{k,1,+}) + |v_k|^2\Theta(-E_{k,1,-})) \\ + \partial\xi_{k\downarrow}(|u_k|^2\Theta(-E_{k,2,+}) + |v_k|^2\Theta(-E_{k,2,-}))\end{aligned} \tag{A36}$$

How does this looks like in the 2x2 case? Consider:

$$H = \begin{pmatrix} \xi_k & -\Delta_k \\ -\Delta_k^* & \xi_k \end{pmatrix} \tag{A37}$$

with eigenvalues:

$$E_{k,\pm} = \pm\sqrt{\xi_k^2 + |\Delta_k|^2} \tag{A38}$$

Bdg transformations (equation (54) from https://phy.ntnu.edu.tw/ changmc/Teach/SM/ch04.pdf):

$$U = \begin{pmatrix} u_k & v_k \\ -v_k^* & u_k \end{pmatrix} \tag{A39}$$

and P_k at temperature 0 K:

$$P_k = \begin{pmatrix} \Theta(-E_{k,+}) & 0 \\ 0 & \Theta(-E_{k,-}) \end{pmatrix} \tag{A40}$$

If

$$J = \begin{pmatrix} \partial\xi_k & 0 \\ 0 & \partial\xi_{-k} \end{pmatrix} \tag{A41}$$

We get:

$$\begin{aligned}\langle j\rangle = \partial\xi_{-k}(|u_k|^2\Theta(-E_{k,-}) + |v_k|^2\Theta(-E_{k,+})) \\ + \partial\xi_k(|u_k|^2\Theta(-E_{k,+}) + |v_k|^2\Theta(-E_{k,-}))\end{aligned} \tag{A42}$$

Finite temperatures
Considering previous equations. We substitute $\Theta(-E) \to f(E)$ (where $f(E)$ is the fermi dirac formula), thus we have:

$$\begin{aligned}\langle j\rangle = \partial\xi_{-k\uparrow}(|u_k|^2 f(E_{k,1,-}) + |v_k|^2 f(E_{k,1,+})) \\ + \partial\xi_{-k\downarrow}(|u_k|^2 f(E_{k,2,-}) + |v_k|^2 f(E_{k,2,+})) \\ + \partial\xi_{k\uparrow}(|u_k|^2 f(E_{k,1,+}) + |v_k|^2 f(E_{k,1,-})) \\ + \partial\xi_{k\downarrow}(|u_k|^2 f(E_{k,2,+}) + |v_k|^2 f(E_{k,2,-}))\end{aligned} \tag{A43}$$

SCHRODINGER EQUATION FOR AN ASYMMETRIC SUPERCONDUCTOR, LONDON EQUATIONS AND JOSEPHSON EFFECTS.

Consider the following Schrodinger equation of a charged particle in a magnetic field with an asymmetric energy dissipation:

$$i\partial_t\psi = [\frac{(\hat{p}-q\mathbf{A})^2}{2m} - a(\hat{p}-q\mathbf{A}) + q\phi]\psi \tag{A44}$$

$\hat{p} \to -i\nabla$

$$i\partial_t\psi = [\frac{(-i\nabla-q\mathbf{A})^2}{2m} - a(-i\nabla-q\mathbf{A}) + q\phi]\psi \tag{A45}$$

$$i\partial_t\psi = [-\frac{1}{2m}\nabla^2 + \frac{iq}{2m}\nabla\mathbf{A} + \frac{iq}{2m}\mathbf{A}\nabla + \frac{q^2}{2m}\mathbf{A}^2 + q\phi + ai\nabla + aq\mathbf{A}]\psi \tag{A46}$$

Define action $S = \hbar\theta$ and insert Madelung transformation $\psi(r,t) = \psi_0(r,t)e^{i\theta(r,t)}$
We obtain:

$$i\partial_t\psi = [i\partial_t\psi_0 - \psi_0\partial_t S]e^{iS} \tag{A47}$$

and:

$$(...)\psi = [-\frac{1}{2m}\nabla^2 + \frac{iq}{2m}\nabla\mathbf{A} + \frac{iq}{2m}\mathbf{A}\nabla + \frac{q^2}{2m}\mathbf{A}^2 + q\phi + ai\nabla + aq\mathbf{A}]\psi_0 e^{iS} \tag{A48}$$

Working on previous equations we get:

$$= [\psi_0\frac{(\nabla S - q\mathbf{A})^2}{2m} - \frac{\nabla^2}{2m}\psi_0 - i\frac{1}{2m}(2\nabla\psi_0 + \psi_0\nabla)(\nabla S - q\mathbf{A}) + ia\nabla\psi_0 - a\psi_0\nabla S + aq\mathbf{A}\psi_0]e^{iS} \tag{A49}$$

$$= [\psi_0\frac{(\nabla S - q\mathbf{A})^2}{2m} - \frac{\nabla^2}{2m}\psi_0 - i\frac{1}{2\psi_0}\nabla(\frac{\psi_0^2}{m}(\nabla S - q\mathbf{A}) + ia\nabla\psi_0 - a\psi_0\nabla S + aq\mathbf{A}\psi_0]e^{iS} \tag{A50}$$

Combining real part of previous equations:

$$-\psi_0\partial_t S e^{iS} = [\psi_0\frac{(\nabla S - q\mathbf{A})^2}{2m} - \frac{\nabla^2}{2m}\psi_0 - a\psi_0\nabla S + aq\mathbf{A}\psi_0 + q\phi\psi_0]e^{iS} \tag{A51}$$

Combining imaginary part of previous equations):

$$i\partial_t\psi_0 e^{iS} = -i\frac{1}{2\psi_0}\nabla(\frac{\psi_0^2}{m}(\nabla S - q\mathbf{A})e^{iS} + ia\nabla\psi_0 e^{iS} \tag{A52}$$

Playing with previous equations (dividing ψ_0 and e^{iS}):

$$Real: -\partial_t S = [\frac{(\nabla S - q\mathbf{A})^2}{2m} - \frac{\nabla^2\psi_0}{2m\psi_0} - a\nabla S + aq\mathbf{A} + q\phi] \tag{A53}$$

$$\frac{(\nabla S - q\mathbf{A})^2}{2m} - \frac{\nabla^2\psi_0}{2m\psi_0} - a\nabla S + aq\mathbf{A} + q\phi + \partial_t S = 0 \tag{A54}$$

Neglecting second term on the left side:

$$\frac{(\nabla S - q\mathbf{A})^2}{2m} - a\nabla S + aq\mathbf{A} + q\phi + \partial_t S = 0 \tag{A55}$$

Notice the term $\frac{(\nabla S - q\mathbf{A})^2}{2m} = \frac{1}{2n}\Lambda J_s^2$
From the fact $J_s^2 = n^2q^2v^2 = \frac{nq^2}{m}nmv^2$

with $\Lambda = \frac{m}{nq^2}$
Thus:

$$\frac{1}{2n}\Lambda J_s^2 - a\nabla\theta + aq\mathbf{A} + q\phi + \partial_t\theta = 0 \tag{A56}$$

Let's attribute the second and third term the asymmetric supercurrent countribution:

$$\frac{1}{2n}\Lambda J_s^2 - a(\nabla\theta - q\mathbf{A}) + q\phi + \partial_t\theta = 0 \tag{A57}$$

$$\frac{1}{2n}\Lambda J_s^2 - aq\Lambda J_s + q\phi + \partial_t\theta = 0 \tag{A58}$$

Giving us the energy-phase relation for our asymmetric superconductor:

$$\partial_t\theta + \frac{1}{2n}\Lambda J_s^2 - aq\Lambda J_s + q\phi = 0 \tag{A59}$$

Similarly with previous equations (dividing by i and e^{iS}, multiply ψ_0)

$$Imaginary : \partial_t\psi_0 = a\nabla\psi_0 - \frac{1}{2\psi_0}\nabla(\frac{\psi_0^2}{m}(\nabla S - q\mathbf{A})) \tag{A60}$$

$$2\psi_0\partial_t\psi_0 = 2\psi_0[a\nabla\psi_0] - \nabla(\frac{\psi_0^2}{m}(\nabla S - q\mathbf{A})) \tag{A61}$$

$$\partial_t n = \partial_t\psi_0^2 = 2\psi_0[a\nabla\psi_0] - \nabla(\frac{\psi_0^2}{m}(\nabla S - q\mathbf{A})) \tag{A62}$$

$$\partial_t n = 2a\psi_0\nabla\psi_0 - \nabla(\frac{n}{m}(\nabla S - q\mathbf{A})) \tag{A63}$$

$$\partial_t n = 2a\psi_0\nabla\psi_0 - \nabla(\frac{n}{m}(\nabla\theta - q\mathbf{A})) \tag{A64}$$

From previous equations we can argue that $\nabla\psi_0^2 = 2\psi_0\nabla\psi_0$
thus for asymmetric supercurrent contribution $\partial_t n = \nabla a\psi_0^2 = \nabla an$
This give us the supercurrent density phase relation:

$$J = \frac{qn}{m}\{\nabla\theta - q\mathbf{A}\} + aqn \tag{A65}$$

$$\Lambda J = \frac{am}{q} - \{\mathbf{A} - \frac{1}{q}\nabla\theta\} \tag{A66}$$

London equations
Taking the curl of previous equations we can get the second London equation:
Notice the curl of a gradient is zero.
The curl of a/q doesn't make sense, if we omitted we have original second london equation:

$$\nabla \times \Lambda J = -\nabla \times \mathbf{A} = -\mathbf{B} \tag{A67}$$

Which leads to original Meissner effect:

$$\nabla^2\mathbf{B} = \frac{\mu_0}{\Lambda}\mathbf{B} = \frac{1}{\lambda^2}\mathbf{B}$$
$$\mathbf{B} = B_0 e^{-r/\lambda}$$

For first London equation we take the time derivative of equation previous equations:

$$\partial_t(\Lambda J) = -\{\partial_t\mathbf{A} - \frac{1}{q}\nabla(\partial_t\theta)\} \tag{A68}$$

Inserting equation previous equations
and $\mathbf{E} = -\partial_t \mathbf{A} - \nabla\phi$
gives:

$$\partial_t(\Lambda J) = \mathbf{E} - \frac{1}{nq}\nabla(\frac{1}{2}\Lambda J_s^2 - aqn\Lambda J_s) \tag{A69}$$

Using $\Lambda J = \frac{am}{q} + \Lambda J_s$
We can show $\Lambda J_s^2 = \Lambda J^2 - 2J\frac{am}{q} + \frac{a^2m^2}{\Lambda q^2}$
Thus:

$$\partial_t(\Lambda J) = \mathbf{E} - \frac{1}{nq}\nabla(\frac{1}{2}\{\Lambda J^2 - 2J\frac{am}{q} + \frac{a^2m^2}{\Lambda q^2}\} - aqn\{\Lambda J - \frac{am}{q}\}) \tag{A70}$$

Rewriting, the first London equation is:

$$\partial_t(\Lambda J) = \mathbf{E} - \nabla(\frac{1}{2nq}\Lambda J^2 - 2a\Lambda J - \frac{a^2m}{2q}) \tag{A71}$$

$$\partial_t(\Lambda J) = \mathbf{E} - \nabla(\frac{1}{2nq}\Lambda J^2 - 2a\Lambda J) \tag{A72}$$

Josepshon effect

Incorporating a gauge invariant phase gradient: $\gamma(r,t)$
We can rewrite previous equations as:

$$J = \frac{qn}{m}\{\nabla\theta - \frac{2\pi}{\Phi_0}\mathbf{A}\} + aqn = \frac{qn}{m}\gamma + \frac{2an\pi}{\Phi_0} \tag{A73}$$

and a gauge invarient phase difference:

$$\varphi(r,t) = \int_1^2 \gamma(r,t) = \int_1^2 (\nabla\theta - \frac{2\pi}{\Phi_0}\mathbf{A})d\ell = \theta_2 - \theta_1 - \frac{2\pi}{\Phi_0}\int_1^2 \mathbf{A}d\ell \tag{A74}$$

We expect:

$$J = J(\varphi) \tag{A75}$$
$$J = J(\varphi + 2n\pi) \tag{A76}$$
$$J(0) = J(2n\pi) = aqn \tag{A77}$$

Thus the first josepshon equation:

$$J(\varphi) = J_c sin(\varphi) + aqn \tag{A78}$$

if Josephson effect has time reversal symmetry we require:

$$J(\varphi) = -J(-\varphi) \tag{A79}$$

Clearly it follows:

$$J(\varphi) \neq -J(-\varphi) \tag{A80}$$

To derive the second Josephson equation we take the time derivative

$$\partial_t\varphi = \partial_t\theta_1 - \partial_t\theta_2 - \frac{2\pi}{\Phi_0}\partial_t\int_1^2 \mathbf{A}d\ell \tag{A81}$$

Inserting energy-phase relation equation we get:

$$\partial_t\varphi = -[\frac{1}{2n}\Lambda(J_s^2(2) - J_s^2(1)) - aq\Lambda(J_s(2) - J_s(1)) + q(\phi_2 - \phi_1)] - \frac{2\pi}{\Phi_0}\partial_t\int_1^2 \mathbf{A}d\ell \tag{A82}$$

if there is continuity for J_s

$$\partial_t\varphi = -q(\phi_2 - \phi_1) - \frac{2\pi}{\Phi_0}\partial_t\int_1^2 \mathbf{A}d\ell \tag{A83}$$

$$\partial_t\varphi = \frac{2\pi}{\Phi_0}\int_1^2 (-\nabla\phi - \partial_t\mathbf{A})d\ell \tag{A84}$$

$$\partial_t\varphi = \frac{2\pi}{\Phi_0}\int_1^2 \mathbf{E}d\ell \tag{A85}$$

Which is the original second josephson equation.
Putting in terms of J instead we get:

$$\partial_t\varphi = [\frac{1}{2nq}\Lambda(J^2(2) - J^2(1)) - 2a\Lambda(J(2) - J(1)) + q(\phi_2 - \phi_1)] - \frac{2\pi}{\Phi_0}\partial_t\int_1^2 \mathbf{A}d\ell \tag{A86}$$

Since a is a constant, continuity in J ($J(1) = J(2)$) yields in the following equation. For constant voltage through the junction:

$$\partial_t\varphi = \frac{2\pi}{\Phi_0}V\varphi(t) = \varphi_0 + \frac{2\pi}{\Phi_0}Vt \tag{A87}$$

Summary

Energy-phase relation:

$$\partial_t\theta + \frac{1}{2n}\Lambda J_s^2 - aq\Lambda J_s + q\phi = 0 \tag{A88}$$

Supercurrent density phase relation:

$$J = \frac{qn}{m}\{\nabla\theta - q\mathbf{A}\} + aqn \tag{A89}$$

Meissner effect/ Second London equation (same as symmetric case since curl of a/q is omitted):

$$\nabla \times \Lambda J = -\nabla \times \mathbf{A} = -\mathbf{B} \tag{A90}$$

First London equation:

$$\partial_t(\Lambda J) = \mathbf{E} - \nabla(\frac{1}{2nq}\Lambda J^2 - 2a\Lambda J) \tag{A91}$$

First Josephson equation:

$$J(\varphi) = J_c sin(\varphi) + aqn \tag{A92}$$

Second Josepshon equation (same as symmetric case assuming a is the same constants for J(1) and J(2)):

$$\partial_t\varphi = \frac{2\pi}{\Phi_0}\int_1^2 \mathbf{E}d\ell \tag{A93}$$

JOSEPSHON APPLICATIONS FOR ASYMMETRIC SUPERCONDUCTORS

Applications of Josepshon equations

To avoid notation confusion we write $n \to \rho$
We also decide to keep all summation indeces the same to avoid over used of variables.
It is understood that they are not necessarily the same. We can write more generally:

$$J(\varphi) = J_c sin(\varphi) + aq\rho + \sum_{m=2}^{\infty} J_m sin(m\varphi) + \sum_{m=1}^{\infty} J_m cos(m\varphi) \tag{A94}$$

Since time reversal symmetry is violated that is $J(\varphi) \neq -J(-\varphi)$

DC Josephson effect

In the absence of a potential difference we know $V = 0$
Clearly, when $\varphi = \theta_2 - \theta_1 = 0$ we get a nonzero current:

$$J = aq\rho \tag{A95}$$

Given a nonzero constant phase $\varphi \neq 0$ we get the leading terms:

$$J = J_c sin(\varphi) + J_m cos(\varphi) + aq\rho \tag{A96}$$

AC Josephson effect

For a constant voltage drop across the junction, V, becomes:

$$\partial_t \varphi = \frac{2\pi}{\Phi_0} V \tag{A97}$$

Giving:

$$\varphi(t) = \varphi_0 + \frac{2\pi}{\Phi_0} Vt \tag{A98}$$

Inserting φ results:

$$J(t) = J_c sin(\frac{2\pi}{\Phi_0} Vt) + aq\rho + \sum_{m=2}^{\infty} J_m sin(m\frac{2\pi}{\Phi_0} Vt) + \sum_{m=1}^{\infty} J_m cos(m\frac{2\pi}{\Phi_0} Vt) \tag{A99}$$

keeping leading terms:

$$J(t) = J_c sin(\frac{2\pi}{\Phi_0} Vt) + J_m cos(\frac{2\pi}{\Phi_0} Vt) + aq\rho \tag{A100}$$

Energy in a Basic Junction

We can define de energy as:

$$W = \int_0^{t_0} JV dt \tag{A101}$$

Thus:

$$W = \int_0^{t_0} (J_c sin(\varphi) + J_m cos(\varphi) + aq\rho)(\frac{\Phi_0}{2\pi}\frac{d\varphi}{dt}) dt \tag{A102}$$

$$W = \frac{\Phi_0}{2\pi} \int_0^{\varphi'} (J_c sin(\varphi) + J_m cos(\varphi) + aq\rho) d\varphi \tag{A103}$$

$$W = \frac{\Phi_0}{2\pi} [J_c(1 - cos\varphi') + J_m sin\varphi' + aq\rho\varphi'] \tag{A104}$$

Inverse AC Josephson effect
In this scenario, the Josephson phase takes the form of $\varphi(t) = \varphi_0 + n\omega t + asin(\omega t)$. Consider

$$V = \frac{\Phi_0}{2\pi}\partial_t\varphi \tag{A105}$$

Thus:

$$V = \frac{\Phi_0\omega}{2\pi}(n + acos(\omega t)) \tag{A106}$$

Interting previous equations results:

$$J(t) = J_c sin(\varphi_0 + n\omega t + asin(\omega t)) + aq\rho + \sum_{m=2}^{\infty} J_m sin(m(\varphi_0 + n\omega t + asin(\omega t))) + \sum_{m=1}^{\infty} J_m cos(m(\varphi_0 + n\omega t + asin(\omega t))) \tag{A107}$$

keeping leading terms:

$$J(t) = J_c sin(\varphi_0 + n\omega t + asin(\omega t)) + J_m cos(\varphi_0 + n\omega t + asin(\omega t)) + aq\rho \tag{A108}$$

Taking a close look to the first term of the equation:

$$J_c sin(\varphi_0 + n\omega t + asin(\omega t)) = J_c Im[e^{i(\varphi_0 + n\omega t + asin(\omega t))}] \tag{A109}$$

$$... = J_c Im[e^{i(\varphi_0 + n\omega t)} e^{iasin(\omega t)}] \tag{A110}$$

Using the fact:

$$exp(iasin(\omega t)) = J_0(a) + 2\sum_{k=1}^{\infty} J_{2k}(a)cos(2k\omega t) + 2i\sum_{k=0}^{\infty} J_{2k+1}(a)sin(2k+1)\omega t \tag{A111}$$

$$= \sum_{k=-\infty}^{\infty} J_k(a)cos(k\omega t) + i\sum_{k=-\infty}^{\infty} J_k(a)sin(k\omega t) \tag{A112}$$

Since $J_k(a) = (-1)^k J_{-k}(a)$ we can drop odd k components in the first sum, and even k components in the second sum.

$$... = J_c Im[e^{i(\varphi_0 + n\omega t)}(\sum_{k=-\infty}^{\infty} J_k(a)cos(k\omega t) + i\sum_{k=-\infty}^{\infty} J_k(a)sin(k\omega t))] \tag{A113}$$

$$... = J_c Im[e^{i(\varphi_0 + n\omega t)}(\sum_{k=-\infty}^{\infty} J_k(a)e^{ik\omega t})] \tag{A114}$$

$$... = J_c Im[(\sum_{k=-\infty}^{\infty} J_k(a)e^{i(\varphi_0 + n\omega t + k\omega t)})] \tag{A115}$$

$$... = J_c Im[(\sum_{k=-\infty}^{\infty} J_k(a)e^{i(\varphi_0 + n\omega t + k\omega t)})] \tag{A116}$$

$$... = J_c(\sum_{k=-\infty}^{\infty} J_k(a)sin(\varphi_0 + n\omega t + k\omega t) \tag{A117}$$

Now we take a close look at the second term of the equation:

$$J_m cos(\varphi_0 + n\omega t + asin(\omega t)) = J_m Re[e^{i(\varphi_0 + n\omega t + asin(\omega t))}] \tag{A118}$$

With similar argument we get:

$$... = J_m Re[(\sum_{k=-\infty}^{\infty} J_k(a) e^{i(\varphi_0 + n\omega t + k\omega t)})] \tag{A119}$$

$$... = J_m(\sum_{k=-\infty}^{\infty} J_k(a) cos(\varphi_0 + n\omega t + k\omega t)) \tag{A120}$$

Inserting previous equations gives:

$$J(t) = J_c(\sum_{k=-\infty}^{\infty} J_k(a) sin(\varphi_0 + n\omega t + k\omega t) + J_m(\sum_{k=-\infty}^{\infty} J_k(a) cos(\varphi_0 + n\omega t + k\omega t)) + aq\rho \tag{A121}$$

To avoid confusion between Bessel functions, $J_k(a)$ and supercurrent J we write $J \to I$
Also asymmetric constant $a \to \alpha$

$$I = I_c(\sum_{k=-\infty}^{\infty} J_k(a) sin(\varphi_0 + n\omega t + k\omega t) + I_m(\sum_{k=-\infty}^{\infty} J_k(a) cos(\varphi_0 + n\omega t + k\omega t)) + \alpha q\rho \tag{A122}$$

GINZBURG-LANDAU THEORY

We start with the expression of free enthalpy g_s for an asymmetric superconductor:

$$g_s = g_n + \alpha|\Psi|^2 + \frac{1}{2}\beta|\Psi|^4 + \frac{1}{2\mu_0}|\mathbf{B}_e - \mathbf{b}|^2 + \frac{1}{2m}|(-i\nabla - q\mathbf{A})\Psi|^2 + a\Psi^*(-i\nabla - q\mathbf{A})\Psi + ... \quad \text{(A123)}$$

We minimize the free enthalpy $G_s = \int_V g_s dV$ with respect to $\delta\Psi^*$ and $\delta\Psi$

$$\delta G_s = \int_V dV\{[(\alpha\Psi^* + \beta\Psi^*|\Psi|^2 + \frac{1}{2m}\Psi^*(-i\nabla - q\mathbf{A})^2 + a\Psi^*(-i\nabla - q\mathbf{A}))\Psi]\delta\Psi^* + c.c\} = 0 \quad \text{(A124)}$$

Clearly, the first Ginzburg-Landau equation is:

$$0 = \alpha\Psi + \beta|\Psi|^2\Psi + \frac{1}{2m}(-i\nabla - q\mathbf{A})^2\Psi + a(-i\nabla - q\mathbf{A}))\Psi \quad \text{(A125)}$$

Now, we perform the minimization of G_s with respect to $\delta\mathbf{A}$

$$\delta g_s = g_s(r, t, \mathbf{A} + \delta\mathbf{A}) - g_s(r, t, \mathbf{A}) \quad \text{(A126)}$$

$$\delta g_s = -\frac{q}{m}(-i\Psi^*\nabla\Psi + i\Psi\nabla\Psi^* + 2q|\Psi|^2\mathbf{A})\delta\mathbf{A} + \frac{1}{\mu_0}(\nabla \times \delta\mathbf{A})(\nabla \times \mathbf{A}) + aq|\Psi|^2\delta\mathbf{A} \quad \text{(A127)}$$

$$\delta g_s = -\frac{q}{m}(-i\Psi^*\nabla\Psi + i\Psi\nabla\Psi^* + 2q|\Psi|^2\mathbf{A})\delta\mathbf{A} + \frac{1}{\mu_0}(\nabla^2\mathbf{A}) + aq|\Psi|^2\delta\mathbf{A} \quad \text{(A128)}$$

We can show $J = -\frac{1}{\mu_0}\nabla^2\mathbf{A}$
Thus:

$$\delta G_s = \int_V dV\{\frac{qi}{m}(\Psi^*\nabla\Psi - \Psi\nabla\Psi^*) + \frac{q^2}{m}|\Psi|^2\mathbf{A} - J + aq|\Psi|^2\}\delta\mathbf{A} = 0 \quad \text{(A129)}$$

Yielding in the Second Ginzburg-Landau equation:

$$J = \frac{qi}{2m}(\Psi\nabla\Psi^* - \Psi^*\nabla\Psi) - \frac{q^2}{m}|\Psi|^2\mathbf{A} - aq|\Psi|^2 \quad \text{(A130)}$$

CALCULATING THE SUPERCURRENT ON AN ASYMMETRIC 3D LATTICE

Hamiltonian Matrix:

$$\hat{H} = \begin{pmatrix} \xi_{k\uparrow} & 0 & \Delta_k & 0 \\ 0 & \xi_{k\downarrow} & 0 & \Delta_k \\ \Delta_k^* & 0 & -\xi_{-k\downarrow} & 0 \\ 0 & \Delta_k^* & 0 & -\xi_{-k\uparrow} \end{pmatrix} \tag{A131}$$

with eigenvalues:

$$E_{k,1,\pm} = \frac{1}{2}(\xi_{k\uparrow} - \xi_{-k\downarrow} \pm \sqrt{(\xi_{k\uparrow} + \xi_{-k\downarrow})^2 + 4|\Delta_k|^2}) \tag{A132}$$

$$E_{k,2,\pm} = \frac{1}{2}(\xi_{k\downarrow} - \xi_{-k\uparrow} \pm \sqrt{(\xi_{k\downarrow} + \xi_{-k\uparrow})^2 + 4|\Delta_k|^2}) \tag{A133}$$

We define:

$$\langle j \rangle = tr[U_k P_k U_k^\dagger \hat{J}_k] \tag{A134}$$

Where U is the unitary matrix obtained from the diagonalization of our Hamiltonian (1).
P_k is the projection operator defined as:

$$P_k = \begin{pmatrix} f(-E_{k,1,+}) & 0 & 0 & 0 \\ 0 & f(-E_{k,2,+}) & 0 & 0 \\ 0 & 0 & f(-E_{k,1,-}) & 0 \\ 0 & 0 & 0 & f(-E_{k,2,-}) \end{pmatrix} \tag{A135}$$

Where f is the Fermi-Dirac function. i.e.:

$$f(E) = \frac{1}{e^{\frac{(E-\mu)}{\kappa T}} + 1} \tag{A136}$$

The supercurrent operator is defined as:

$$\hat{J} = \begin{pmatrix} \partial\xi_{k\uparrow} & 0 & 0 & 0 \\ 0 & \partial\xi_{k\downarrow} & 0 & 0 \\ 0 & 0 & \partial\xi_{-k\uparrow} & 0 \\ 0 & 0 & 0 & \partial\xi_{-k\downarrow} \end{pmatrix} \tag{A137}$$

We define the total current density as:

$$\langle J \rangle = \frac{1}{V} \sum_k \langle j_k \rangle \tag{A138}$$

By considering periodic boundary conditions ($k = \frac{2\pi n}{L}$). We get:

$$\langle J \rangle = \frac{1}{V} \sum_n \langle j_k \rangle \tag{A139}$$

In 3-D we get the triple summation:

$$\langle J \rangle = \frac{1}{V} \sum_{n_x n_y n_z} \langle j_k \rangle \tag{A140}$$

Note that the momentum k within the first Brillouin zone ($-\frac{\pi}{a} < k < \frac{\pi}{a}$) and integer n. n has to take values of $n - \frac{N}{2} = 1, 2..., N-1, N = n - \frac{L}{2} = 1, 2..., L-1, L$ (for $L = Na \because a = 1 \implies L = N$).

Asymmetric lattice model with superconductivity Hamiltonian Meeting notes

Consider the derived Hamiltonian and energy dispersion from previous work:

$$H = \sum_{k,\sigma} \xi_k c_{k\sigma}^\dagger c_{k\sigma} + VN \tag{A141}$$

$$H = \sum_{k,\sigma} (-tcos(ka + \theta)) c_{k\sigma}^\dagger c_{k\sigma} + VN \tag{A142}$$

Consider the following relative Gauge transformation $k = k' - \frac{\theta}{a}$, then the Hamiltonian becomes:

$$H' = \sum_{k,\sigma}(-tcos(k'a))c^\dagger_{k\sigma}c_{k\sigma} + VN \tag{A143}$$

which recovers inversion symmetry.
To overcome this we consider a lattice with a (even sites) and b (odd sites) for 1D case. For higher dimensions we consider a site a to be neighbor of every other b site. We can observe figure below. Note we still have undistinguishable atoms

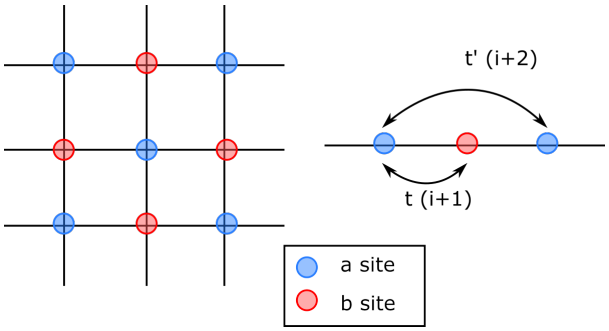

Note now we can consider 2 types of hopping terms. Namely, $t, t' \in \mathbb{C}$ (For TR symmetry breaking). Thus we have:

$$H = -\frac{1}{2}\sum_{i,\sigma}\sum_{\delta}(te^{i\theta}c^\dagger_{i\sigma}c_{i+\delta,\sigma} + te^{-i\theta}c^\dagger_{i+\delta,\sigma}c_{i\sigma}$$

$$+ t'e^{i\varphi}c^\dagger_{i\sigma}c_{i+2\delta,\sigma} + t'e^{-i\varphi}c^\dagger_{i+2\delta,\sigma}c_{i\sigma}) + VN \tag{A144}$$

Hence the energy dispersion is:

$$\xi_k = tcos(ka+\theta) + t'cos(2ka+\varphi) \tag{A145}$$

Under the same relative Gauge transformation (shifting k by θ) we get:

$$\xi_k = tcos(k'a) + t'cos(2k'a+\varphi-2\theta) \tag{A146}$$

Inversion symmetry is still violated. Note that new hopping terms shouldn't add anything qualitatively new (e.i. $t'' = i+3$).
Now we observe the BCS Hamiltonian

$$H = \sum_{k,\sigma}\xi_k c^\dagger_{k\sigma}c_{k\sigma} - \sum_k(\Delta_k c^\dagger_{k\uparrow}c^\dagger_{-k\downarrow} + \Delta^*_k c_{-k\downarrow}c_{k\uparrow}) + \sum_k \Delta_k \left\langle c^\dagger_{k\uparrow}c^\dagger_{-k\downarrow}\right\rangle \tag{A147}$$

Considering the previously derived asymmetric energy dispersion:

$$\xi_k = tcos(ka+\theta) + t'cos(2ka+\varphi) \tag{A148}$$

Apply a Gauge Transformation $ka+\theta \to k'a$. Define $\tilde{\theta} = \phi - 2\theta$.

$$\xi_k = tcos(ka) + t'cos(2ka+\tilde{\theta}) \tag{A149}$$

Generalizing in 3-D

$$\xi_k = tcos(k_xa) + t'cos(2k_xa+\tilde{\theta}_x) + tcos(k_ya) + t'cos(2k_ya+\tilde{\theta}_y) \tag{A150}$$

$$+tcos(k_za) + t'cos(2k_za+\tilde{\theta}_z) \tag{A151}$$

With the derivative:

$$\partial\xi_k = -atsin(ka) - 2at'sin(2ka+\tilde{\theta}) \tag{A152}$$

and

$$\xi_{-k} = tcos(-ka) + t'cos(-2ka+\tilde{\theta}) \tag{A153}$$

$$\partial\xi_{-k} = atsin(-ka) + 2at'sin(-2ka+\tilde{\theta}) \tag{A154}$$

Consider the following parameters for a numerical calculation of the supercurrent density in the x-direction. $L_z = 20, t = 1, t' = \frac{1}{2}, \theta = \{\frac{\pi}{6}, \frac{2\pi}{6}, \frac{3\pi}{6}\}, T = 1, \kappa = 1, \mu = 0, a = 1, \Delta = .2, k = \frac{2\pi n}{L}, n + \frac{L}{2} = 1, 2...L-1, L.$ The following plot is generated.
Note to calculate supercurrent in a linear direction we compute the derivatives withing the supercurrent operator in the desired direction. That is for x-direction:

$$\hat{J}_x = \begin{pmatrix} \partial\xi_{k_x\uparrow} & 0 & 0 & 0 \\ 0 & \partial\xi_{k_x\downarrow} & 0 & 0 \\ 0 & 0 & \partial\xi_{-k_x\uparrow} & 0 \\ 0 & 0 & 0 & \partial\xi_{-k_x\downarrow} \end{pmatrix} \tag{A155}$$

Varying different lattice sizes we get the following figure

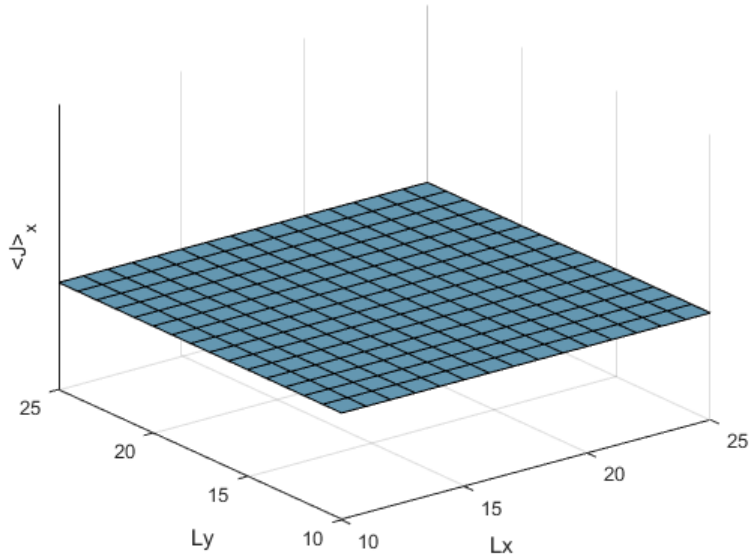

Then, I explore the dependence on θ. With same previous parameters.

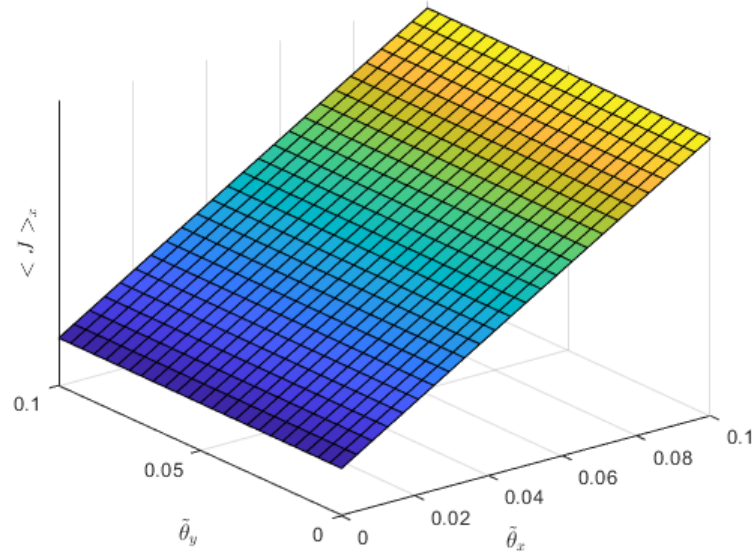

COMPLEX ENERGY GAP AND RING GEOMETRY

Future work, Investigate ring geometry in superconductors to explore the possibility of calculating numerically the supercurrent density in asymmetric ring superconductors.
Consider a complex energy gap.

$$H = \begin{pmatrix} \xi_k & 0 & \Delta_0 + \Delta_z & \Delta_x - i\Delta_y \\ 0 & \xi_k & \Delta_x + i\Delta_y & \Delta_0 - \Delta_z \\ \Delta_0^* + \Delta_z^* & \Delta_x^* - i\Delta_y^* & -\xi_{-k} & 0 \\ \Delta_x^* + i\Delta_y^* & \Delta_0^* - \Delta_x^* & 0 & -\xi_{-k} \end{pmatrix} \tag{A156}$$